Calcif Tissue Int (1991) 48:341–352

Calcified Tissue International

A Correlation between the Distribution of Biological Apatite and Amino Acid Sequence of Type I Collagen

Murray E. Maitland[1] and A. Larry Arsenault[2]

[1]Sports Medicine Centre, University of Calgary, Calgary, Alberta, Canada; and [2]Electron Microscopic Facility, Faculty of Health Sciences, 1200 Main Street West, McMaster University, Hamilton, Ontario, Canada L8N 3Z5

Summary. We have determined the localization of apatite within type I collagen fibrils of calcifying turkey leg tendons by both bright field and selected-area dark field (SADF) electron microscopy and have compared this to computer-modeled, chick type I collagen amino acid sequence data. Apatite crystals occur in both the gap and overlap zones at early stages of mineralization in an asymmetric pattern that corresponds to the polarity, N- to C- orientation, of the collagen molecule. Based on comparisons with computer-generated models of known amino acid sequence of collagen, it was determined for early stages of mineral deposition that apatite is restricted by areas of high hydrophobicity. The gap zone is less hydrophobic than the overlap zone on average but each of these zones had areas of high hydrophobicity that correlated with sites of low localization of mineral. Possible interactions between hydrophobic regions and the process of mineral deposition are discussed.

Key words: Biological apatite — Type I collagen — Mineralization — Electron microscopy — Computer modeling.

Type I collagen provides structural integrity to numerous connective tissues and is directly involved in the mineralization of bone, dentin, and turkey leg tendons. The collagen molecule is a semiflexible rod 300 nm in length formed by two α1(I) and one α2(I) amino acid chains [1, 2]. These molecules have a triple helical portion (1014 amino acid residues) and small N- and C- terminal, nonhelical portions. Hodge and Petruska [3] showed that the collagen molecules are longitudinally organized in a regular 67 nm, D-staggered fashion which gives rise to its axial period. The molecules are linearly arranged such that there is a 35 nm separation between adjacent ends and each molecule is staggered to its lateral neighbor by 67 nm, corresponding to 234 amino acid residues [4]. The repeating D period of the collagen fibril was envisioned as having two regions: a densely packed overlap region, .4D in length, and a "gap" region, .6D in length, where there would be potential space as the result of the separation between longitudinally arranged molecules. Hodge and Petruska [3] suggested that the gap region would be the preferential location of apatite crystals during mineralization due to the space available for crystal growth. The regular D-stagger of the collagen molecules also results in the periodic localization of amino acids with specific structural and histochemical implications [5]. Meek et al. [6] were able to integrate the known amino acid sequence, structural information, and the staining patterns of type I collagen to model the localization of individual amino acids within the fibril. A high correlation coefficient ($r = 0.926$) was found between the electron-optical density of positively stained collagen and the theoretical density of their model. Subsequent studies have used the amino acid sequence data of collagen to determine the localization of electron-dense stains with specific classes of amino acids [7–10]. An analogous approach can be used to understand the impregnation of mineral into collagen fibrils by the localization of apatite crystals relative to the known amino acid composition. In this present study, in addition to heavy metal staining, electron density and diffracted electrons of ap-

Offprint requests to: Dr. Larry Arsenault

atite are analyzed and compared with models of the collagen amino acid sequence.

Corroborating the suggestion by Hodge and Petruska [3], several authors have reported the occurrence of apatite in the gap zone and its exclusion from the overlap zone of type I collagen [11, 12]. Other authors describe the initial localization of mineral to be exclusively in the gap zone followed by progressive spread throughout the overlap zone [13]. Recent information indicates that the earliest detectable apatite crystals are localized within the overlap zone in addition to the gap zone [14] and that the proportion of mineral in the gap and overlap zones changes as mineralization proceeds [15]. Image analysis utilizing fast Fourier transformations has been used to separate the axial repeat bandings of mineralized collagen from the more random, nonrepeating distribution of mineral [16]; these combined procedures have directly revealed an integrated intrafibrillar mineral distribution that is not confined simply to the gap zone. Moreover, many questions remain concerning the role of collagen structure in the mechanism of biological apatite deposition, whether this is a passive association, an interactive process, or whether an intermediary is the dominant force. Many of these studies have used the mineralized turkey tendon instead of bone tissue proper because of the tendon's high degree of collagen fibril alignment, thereby permitting ease of sequential analyses of the mineralization process along individual fibrils.

The present study was undertaken to investigate the intrafibrillar localization of apatite in relation to the amino acid sequence of type I collagen in the turkey leg tendon. To achieve this goal, ultrastructural data of mineralized and nonmineralized collagen fibrils were compared to the primary ordering of computer-modeled amino acid sequences of type I collagen; the secondary and tertiary chain ordering of these amino acids are not accounted for in this computer model. This study revealed an asymmetric and subperiodic organization of apatite within the collagen D period which correlates with the polarized N- to C- direction of the collagen fibril as determined by the staining pattern. A reverse relationship between the localization of apatite and the localization of hydrophobic amino acids was found to be evident in both the gap and overlap zones. Our primary conclusion is that the hydrophobic effect, which is important to collagen structure, also serves to influence the distribution of apatite. The distribution of the crystals in the turkey leg tendon therefore does not appear to be determined by the gap region in collagen fibrils but could be controlled by other collagenous or noncollagenous influences.

Materials and Methods

Electron Microscopy

Excised leg tendons from 14-week-old domestic turkeys were placed in 100% glycerol for 3 hours. Areas of interest near the mineralization front were removed and placed in a graded series of glycerol/methanol and then embedded in Spurr's resin. Thin sections were cut in longitudinal planes along the tendons with a diamond knife. In order to visualize collagen banding, sections were stained with 1% aqueous phosphotungstic acid (PTA) at pH 3.2 and 1% aqueous uranyl acetate (UA) at pH 4.2 for 10 minutes each. Although this staining method produces the conventional banding pattern of type I collagen, it was found to demineralize turkey leg tendons [14]. In order to visualize the molecular orientation of collagen fibrils by analysis of their banding patterns and to maintain the native distribution of apatite, sections were stained with 1% UA in 100% ethanol for 3–5 minutes. Preservation of apatite with alcoholic UA staining was assessed by electron diffraction analysis. Bright field electron microscopy was performed on both stained and unstained sections using a Philips 300 electron microscope operating at 80 kV. This microscope was also used for tilt-beam dark field to collect diffracted electrons from apatite crystals present within the collagen fibrils of mineralized tendons. This technique of selected-area dark field (SADF) imaging has been previously described [14] and used here to collect diffracted electrons from the c-axial lattice planes of apatite which correspond to the (002) d spacing. The collection and imaging of these electrons provide for the direct and specific visualization of apatite crystals within collagen at the resolution of the electron microscope.

Densitometry

Images of mineralized collagen were digitized and entered into a computer (Kontron IBAS; Etching, West Germany). These 512 × 512 matrices were then averaged along the lateral direction of the mineral cross banding, thereby reducing localized variations in mineral distribution. The filtered images were then used for linear densitometric tracings along the mineral repeats. Grey values ranging from 0 to 255, black to white, were then plotted.

Computer Modeling

The system of modeling amino acid sequence in collagen fibrils used here is an adaptation of the system developed by Meek et al. [6]. The amino acid sequences for α1(I) [17] and α2(I) [18] chick collagen were translated into single letter codes and entered each as a single string into a text editor. Chick collagen sequences were used because amino acid data for turkey is unavailable at this time. The results when using either turkey or chick data are expected to differ only minimally because there is a large degree of sequence homology between species [18]. These single strings were organized into repeating D-units, 234 amino acids in length and 5 molecules in width. The relative positions of the two α1(I) and the α2(I) chains were assumed to be α1-α2-α1 [9] and the telopeptides were assumed to be linear. The repeating units were then stacked to simulate 4 D units in length by 50 molecules in width. In order to represent the charged amino acids responsible for the positive staining pattern

of collagen, aspartic acid, glutamic acid, lysine, arginine, and histidine were left in their positions while all other amino acids were replaced by spaces. The resultant distribution was reduced by computer and then further reduced photographically to the equivalent size of electron microscopic images. The molecular orientation of collagen stained with alcoholic UA was determined by comparisons with a theoretical model of the distribution of negatively charged amino acids (aspartic acid and glutamic acid). The periodic distribution of the hydrophobic amino acids having long side-chains, phenylalanine, methionine, valine, leucine, and isoleucine has been considered to be important in fibril structure [19]. These hydrophobic amino acids were selected and then reduced to the scale of mineralized collagen fibrils for direct visual comparisons. The reverse contrast of this image represents areas low in hydrophobic groups as black and areas high in hydrophobic groups as white.

A linear estimate of the hydrophobicity at a single D period repeating unit of five molecules (15 peptides) was calculated by first assigning a hydropathy index value [20] for isoleucine, leucine, valine, phenylalanine, methionine, and alanine; all other residues were assigned a value of zero. Beginning at the first residue of the N- terminus (position 1), and advancing in the C-direction to position 234, the hydrophobicity values of the 15 corresponding positions of the laterally adjacent peptides were summed. Each of these 234 values were in turn averaged with five adjacent values on either side and plotted against the position number. A three-dimensional representation of hydrophobicity for this same segment was obtained by plotting the position number (x-axis), the peptide number (y-axis), and hydrophobic value (z-axis). This hydrophobic value was derived from the average of the three adjacent values on either side of the residue. Grey levels were assigned to the three-dimensional plot with white representing the highest degree of hydrophobicity and black the lowest.

Results

Longitudinal planes of section through nonmineralized portions of stained tendons reveal tightly apposed type I collagen fibrils aligned in a parallel fashion (Fig. 1a). The pronounced axial repeat of these fibrils consists of alternating light and dark regions which are due to the specific staining properties of the highly ordered collagen molecules. At a higher magnification (Fig. 1b), each axial repeat is shown to be composed of an asymmetric series of narrow bands which have been given an "a, b, c, d, e" nomenclature [21]. Each band can be identified by its relative staining intensity, width, and spatial relationships to other bands. The intensity, and therefore the fine structure, of these bands varies depending upon the staining methods used; fibrils in Figures 1a and b have been stained with aqueous PTA/UA stains which gives optimal definition to each band. The morphological details of these bands are as follows: the *a bands* (a_1, a_2, a_3, and a_4) are narrow, closely spaced bands that tend not to be clearly delineated; the two *b bands* (b_1 and b_2) are very distinct and well separated, and also have a well-defined border between the adjacent a and c bands, for the *c bands* (c_1, c_2, and c_3), only c_2 is readily apparent whereas the others are faint; the *d band* is an intense single band with well-defined borders; the *e bands* (e_1 and $_2$) are distinct, dense lines narrowly separated from each other, e_2 and a_1 are separated by a narrow lucent space. In Figure 1a, the densely stained regions are due to bands e, a and b and c and d form the light regions. At the molecular level, studies have shown that the gap zone, the distance separating longitudinally arranged collagen molecules, consists of $a_{3,2,1}$, $e_{2,1}$, d, and c_3 and the overlap zone consists of $c_{2,1}$, $b_{2,1}$, and $a_{4,3}$ [3].

The banding pattern of type I collagen represents the distribution and density of charged groups of amino acids; therefore, theoretical models can be constructed from the known amino acid sequence of type I collagen. In our computer-generated model (Fig. 1c) charged amino acids align vertically to give the 'a to e' banding pattern of native collagen fibrils. This model was then scaled and aligned to the stained collagen fibril (Figs. 1b and inset). The registration and intensity of the bands derived by computer modeling correspond to the stained image and permit unambiguous determination of collagen orientation. The N- to C- direction of collagen molecular orientation correlates with the 'e to a' presentation of this asymmetric pattern of bands (Fig. 1b). In this study it was found that adjacent fibrils in turkey tendon may be of the same or of opposite orientation and thus, the determination of molecular orientation within the collagen fibril is critical to the analysis of apatite localization.

Unstained, longitudinal sections at the mineralization front of turkey leg tendons (Fig. 2a) reveal a distinct repeating pattern due to the electron density of apatite crystals. In contrast, nonmineralized regions of the same section do not demonstrate any structural detail. In regions of early mineralization, most electron density occurs in the gap zone; however, electron-dense material is also present in the overlap zone. More specifically, one observes that each zone has a pattern of electron density which is neither random nor homogeneous. The gap zone appears to be delineated, on either side, by an electron-lucent line and within the gap zone is a single asymmetrically positioned lucent area. At this early stage of mineralization, apatite deposition is evident in the midportion of the overlap zone. In regions of increased mineral deposition similar features are observed but the difference in contrast between the gap and overlap zones is less marked. At higher magnification (Fig. 2b), an area showing the early stages of mineralization depicts this pattern of mineral distribution in greater detail. The SADF image

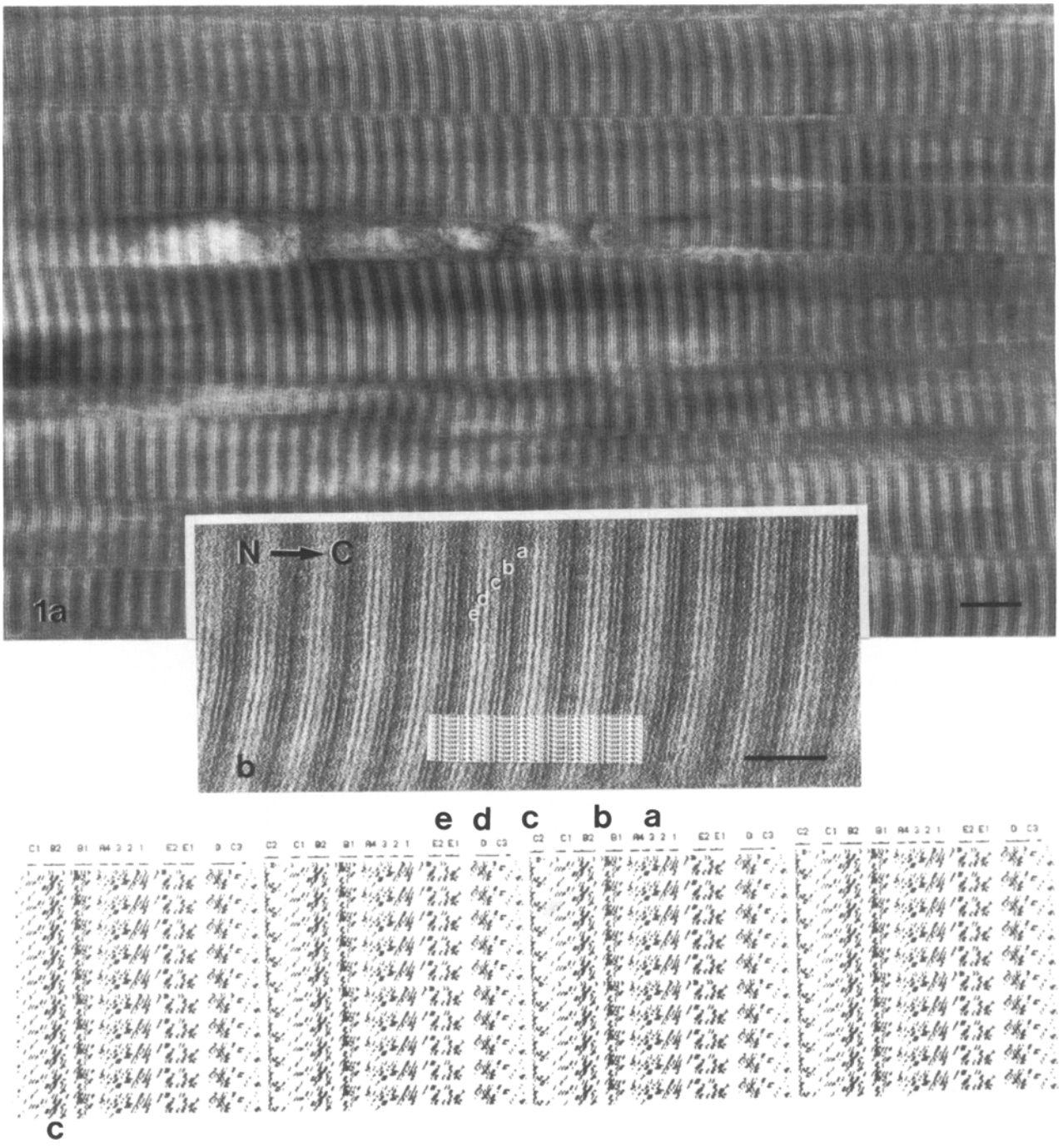

Fig. 1. A comparison between PTA/UA stained collagen and computer displays of collagen amino acid sequence. **(a)** Type I collagen fibrils of the turkey leg tendon viewed in a stained, longitudinally cut thin section. These parallel, axially aligned fibrils possess light and dark repeats throughout their length. **(b)** At a higher magnification each individual repeat is observed to consist of five easily recognizable series of bands which are conventionally labeled "a, b, c, d, and e." This image is presented with its N- to C- molecular orientation extending from left to right (b, inset) A scaled computer-displayed image from c is aligned to the collagen image of b. The banding patterns of both images lie in complete registration. **(c)** A computer-displayed image of positively and negatively charged amino acids is shown in the same molecular orientation as in b. This display provides the spatial distribution and characteristic alignments of these charged amino acids; the resulting bands are labeled from "e to a" indicating that the N- to C-molecular orientation is from left to right. **(a, b)** Stained with aqueous PTA and UA. Bars **(a)** 200 nm; **(b)** 100 nm.

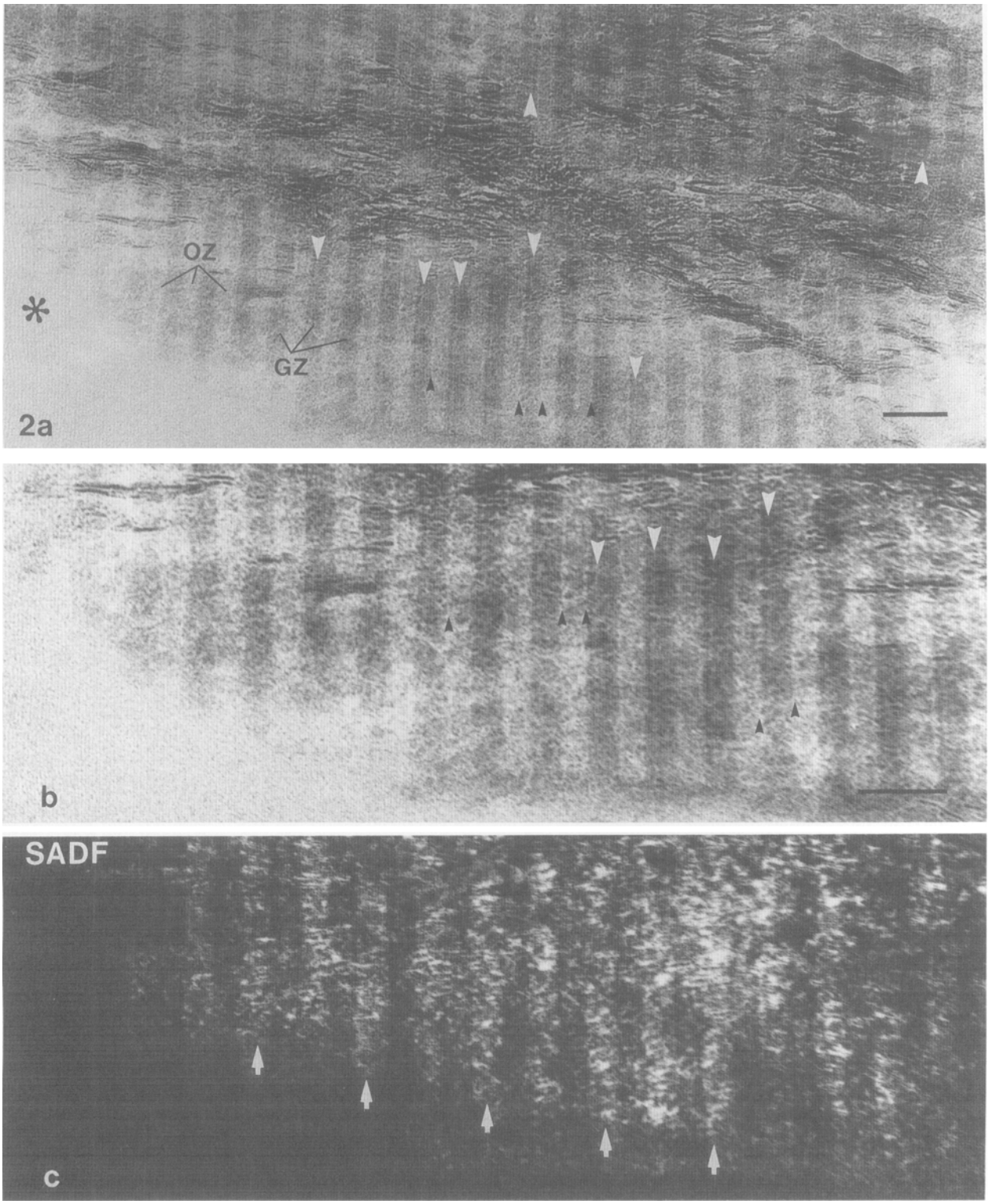

Fig. 2. Mineral distribution in collagen. **(a)** A bright field image of an unstained mineralized portion of a turkey leg tendon showing two collagen fibrils with an inherent banding pattern due to a high mineral content in gap zones (GZ) as compared to less mineral in the interspaced overlap zones (OZ). The mineral has an asymmetric distribution within gap zones as demarcated by a lucent space (white arrowheads). This distribution is consistent within a given fibril but can be oppositely positioned in the adjacent fibril as shown (note the position of the lucent space in the gap zone of two fibrils). Also, the gap zones are bordered on both sides by a narrow lucent space (black arrowheads). Nonmineralized portion of collagen (*). At higher magnification a bright field image **(b)** of a collagen fibril is compared to a selected-area dark field image **(c)** of the same specimen area. **(b)** Lucent spaces in the gap zones (white arrowheads); lucent spaces bordering the gap zone (black arrowheads). Often mineral in the overlap zones appears linearly arranged as centrally positioned, dense bands. **(c)** The dark field image shows the specific localization of apatite crystals (c-axial lengths) which appear as white highlights. The gap zones (arrows) are clearly distinguished from the intervening overlap zones by increased concentrations of apatite. Bars, 100 nm.

specifically identifies and directly visualizes apatite crystals within both gap and overlap zones (Fig. 2c); these c-axially oriented crystals appear in reverse contrast to the bright field image of the same region at the same magnification. It is apparent that the pattern of mineral deposition demonstrated by SADF is the same as by bright field electron microscopy.

In order to correlate the molecular orientation of collagen with the pattern of apatite deposition it is necessary to relate the stained collagen banding pattern of nonmineralized areas with mineralized areas on the same fibril. Certain technical difficulties must be overcome because it is known that aqueous staining procedures demineralize tissue [22]. Therefore, to enhance the fine structure of collagen fibrils and to retain the native distribution of apatite crystals, we stained sections with alcoholic UA. The alcoholic UA staining produced a different banding pattern as compared to the aqueous PTA/UA stains. So to unambiguously determine the molecular orientation of collagen with this UA stain, we have constructed a model of negatively charged amino acids (Fig. 3a). This model was then scaled and aligned to a representative region of a nonmineralized collagen fibril (Figs. 3b and inset). The banding patterns of the stained fibril and the scaled computer model are in registration, thereby enabling the determination of N- to C- molecular orientation which is directed from left to right in this image. Above this collagen fibril is another fibril which has the opposite molecular orientation (Fig. 3b). The b_1 and b_2 bands observed with alcoholic UA staining were similar in appearance to the PTA/UA stained pattern and consisted of a distinct pair of bands within the more electron-dense region of the D period. The c_2 band also retained its characteristic intensity. However, the a, e, and d bands maintained their relative positions but were not as intensely stained as with PTA/UA.

Having established the N- to C- molecular orientation of nonmineralized alcoholic UA stained fibrils, we then determined the molecular orientation of individual fibrils that have both mineralized and nonmineralized portions (Fig. 3c). A nonmineralized collagen fibril, having a well-defined banding pattern with the N- to C- molecular orientation from left to right (Fig. 3d) has been aligned to a nonmineralized portion of Figure 3c in order to clarify the somewhat poorly defined banding of these fibrils. All of the collagen fibrils in Figure 3c have the same N- to C- orientation from left to right. Advancing towards the mineralized portion of the fibrils, the stained banding pattern is gradually replaced by the characteristic pattern of apatite distribution. Electron diffraction analysis from these dense mineralized areas showed the characteristic maxima for biological apatite crystals thereby confirming its presence (data not shown). The distribution of apatite in these gap and overlap zones were precisely the same as was observed for unstained mineralized sections (compare Figs. 2 and 3c). Within the gap zone the asymmetric distribution of mineral is created by a lucent space (Fig. 3c). The positioning of this space is consistent with the N- to C- orientation of the collagen fibril and when apparent is nearest to the N- terminus. It was observed that adjacent mineralized fibrils having opposite orientations have lucent spaces positioned in the gap zone consistent with this opposite polarity.

After determining the N- to C- molecular direction of mineralized collagen fibrils, the nature of this apatite-collagen distribution was further analyzed by comparison to computer models selecting for various amino acid groups such as charged (positive and/or negative charge), polar noncharged, aromatic, and hydrophobic groups. These classes of amino acids were selected because of their influence on collagen structure. Of these, the model having the best fit to the unstained mineralized collagen fibril was the hydrophobic group displayed in both normal and reverse contrast images (Fig. 4a). It was observed from the computer model that there are three regions with high spatial densities of hydrophobic amino acids (which are displayed as white areas in the reverse contrast image). Two of these hydrophobic regions, a_4-a_3 and c_2-c_1, border each side of the gap zone; the third lies asymmetrically positioned in the gap zone between a_1 and e_2 nearer the N-terminus of the collagen molecule. Regions of the collagen molecule containing hydrophobic amino acids with low spatial densities include most of the gap zone; intermediate regions lie within the overlap zone from c_1 to a_4, and within the gap zone from e_1 to c_2. These computer-generated hydrophobic repeats align and correlate with micrographs of unstained mineralized collagen (Figs. 4b and inset). In this set of images it is clearly shown that apatite is restricted from those areas occupied by high spatial densities of hydrophobic amino acid residues.

An averaged grey value plot representing the densities of consecutive gap and overlap zones within early mineralized collagen is shown in Figure 5a. Although the degree of mineralization varies between D periods, elevated grey levels are characteristically positioned within each zone. The higher grey levels correspond to areas of reduced mineral density whereas the lower levels are sites of high mineral density. The first D period of this densitometric plot (Fig. 5b) was aligned to the averaged hydrophobicity for the repeating D unit (Fig. 5c). These aligned plots clearly illustrate the coincident

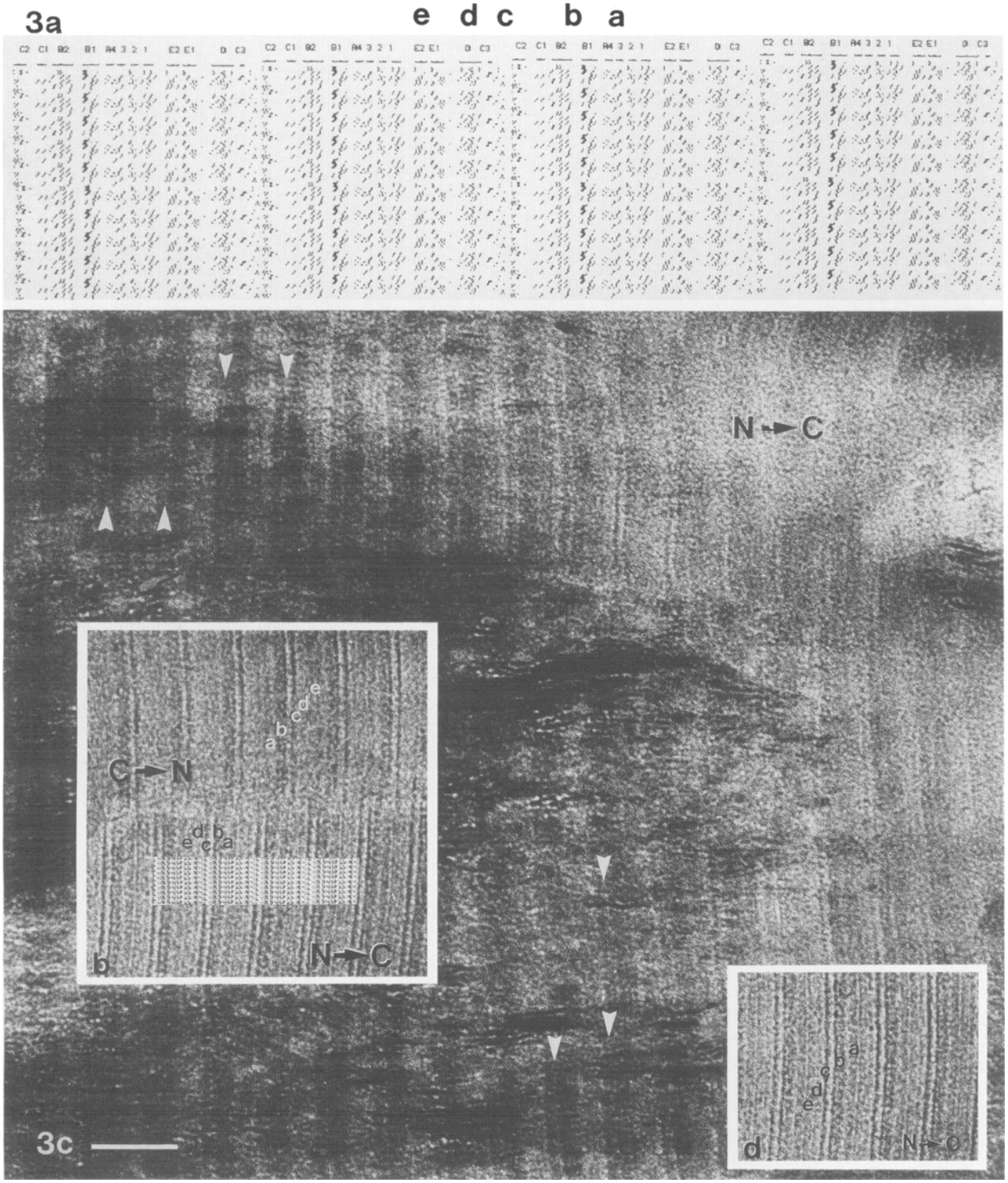

Fig. 3. Analysis of collagen molecular orientation by alcoholic UA staining of mineralized and nonmineralized turkey tendon. **(a)** A computer image displaying the spatial distribution of negatively charged amino acids; the N- to C-molecular orientation is from left to right. **(b)** Two adjacent nonmineralized collagen fibrils stained with alcoholic UA; these fibrils have an opposite N- to C- molecular orientation as indicated by their opposite banding patterns. (b, inset) A scaled computer image of negatively charged amino acids aligned to the fibril having its N- to C- molecular orientation extending from left to right. The banding patterns of the computer image lie in register with those of the fibril image. **(c)** A stained bright field image of collagen fibrils showing a dense mineralized area and a nonmineralized area. The asymmetric positioning of lucent spaces in the gap zones (arrowheads) is nearer the N- terminus. **(d)** Well-defined collagen banding with N- to C- molecular orientation presented from left to right; this banding is in perfect registration with the more poorly defined banding of c. (b, c, d) stained with alcoholic UA. Bar, 100 nm.

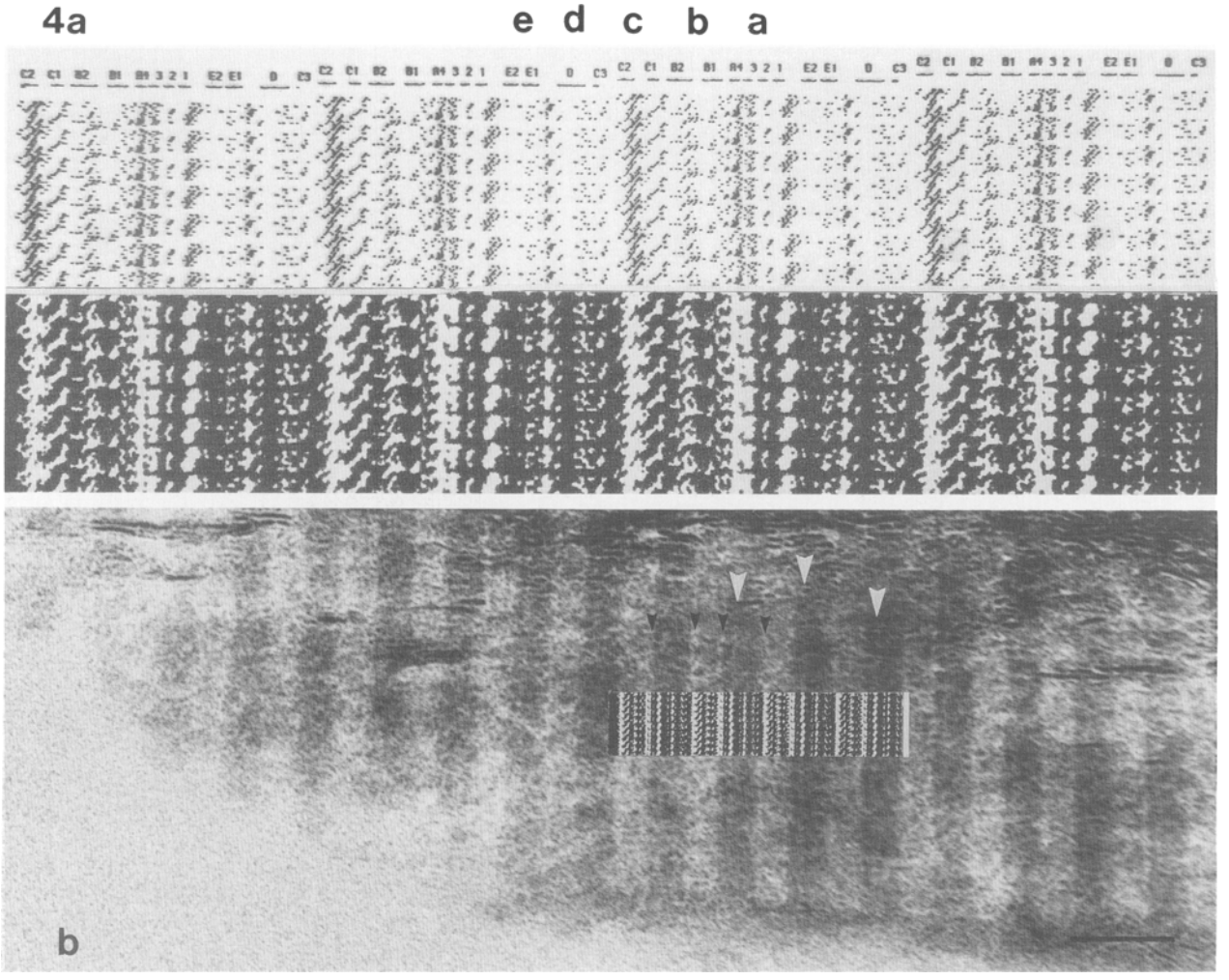

Fig. 4. A comparison of the distribution of hydrophobic amino acids and mineral apatite. **(a)** A computer image of hydrophobic amino acid groups displayed in normal and reverse contrast; the N- to C- molecular orientation is from left to right. **(b)** An unstained mineralized collagen fibril is shown with an aligned and scaled reverse contrast computer image of hydrophobic amino acids (inset). The registration and corresponding densities of the two images coincide. The asymmetrically localized mineral (density) corresponds to regions low in hydrophobic amino acids, whereas areas void of mineral (lucent) correspond to regions high in hydrophobicity. Bar, 100 nm.

rise in grey levels (sites of reduced mineral deposition) and hydrophobicity. This corroborates the alignment of the computer displayed hydrophobic image and the mineral distribution in collagen (Fig. 4b).

The two-dimensional hydrophobic plot (Fig. 5b) does not account for the potential complexities of the spatial relationships (interactions) of amino acids in collagen. To overcome this limitation, three-dimensional graphics were used to represent hydrophobicity within the collagen D period (Fig. 6). In this perspective the position and degree of hydrophobicity are viewed from above with white representing the highest levels and black the lowest. The length of a native collagen molecule is 214 times its width. For graphic purposes, the molecular length has been assigned to be 56 times the width; therefore, the width of each molecule and the gap space are both greatly overrepresented. From this 3-D graphics presentation, three regions of high hydrophobicity are observed to span the width of the D unit—two regions in the overlap zone (c_2-c_1 and a_4-a_3) and one in the gap zone (a_1-e_2). Other regions of both zones vary in levels of hydrophobicity across the D unit giving a highly textured appearance. The spatial distribution of low hydrophobic levels (black to dark grey pixels) corresponds to the sites of early mineral deposition. For example, areas of low hydrophobicity in the overlap zone (c_1-b_1) and the gap zone (a_2-a_1, e_2-e_1, d-c_3, and the gap space) all contain sites of early mineral deposition.

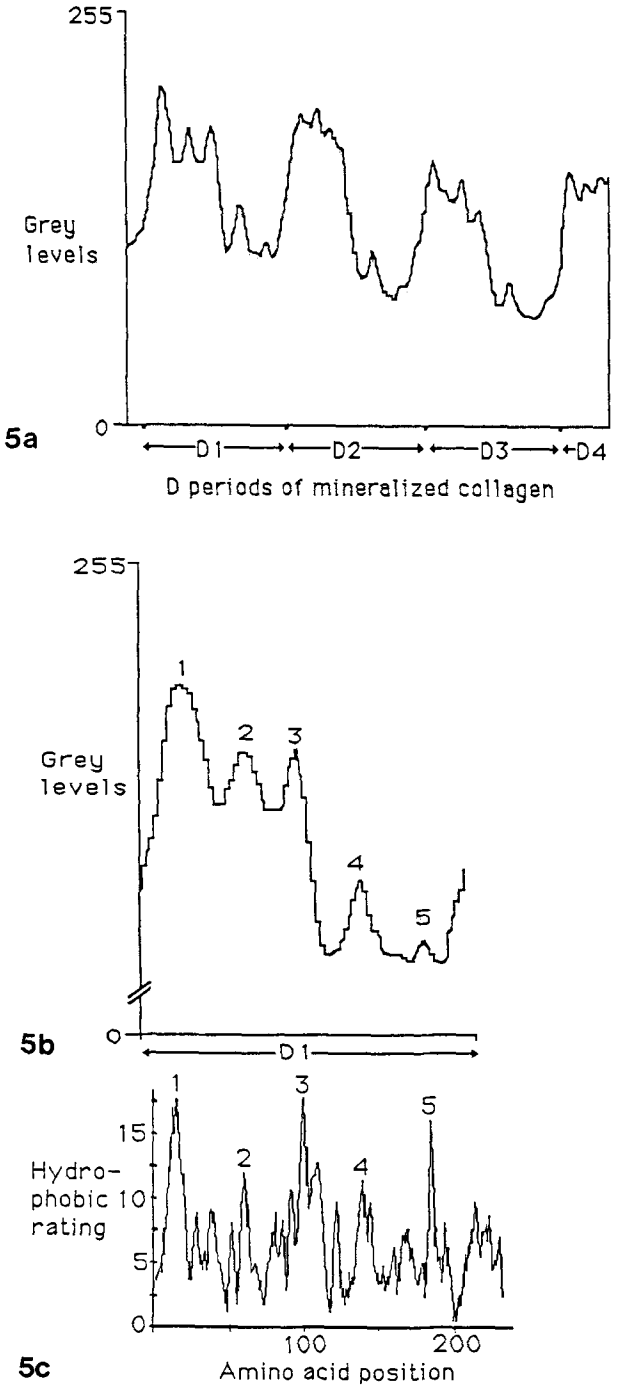

Fig. 5. Comparison of densitometric grey level plots and estimated hydrophobicity values of a D period. **(a)** A grey value plot representing the densities of consecutive gap and overlap zones within early mineralized collagen. Although the degree of mineralization varies between D periods, elevated grey levels are characteristically positioned within each zone. The higher grey levels correspond to areas of reduced mineral deposition and the lower levels are sites of high mineral deposition. **(b)** The first D period of this densitometric plot was aligned to **(c)** the averaged hydrophobicity for the repeating D unit. These aligned plots clearly illustrate the coincident rise in grey levels, labeled 1–5 (sites of reduced mineral deposition) and hydrophobicity.

Discussion

The ordered distribution of apatite crystals in type I collagen has been an important subject of study because of the interactive role of mineral and collagen in producing the biomechanical properties of skeletal tissues. This distribution has long been viewed to reflect the intrinsic nature of collagen structure. However, at this time our knowledge of how apatite crystals may interact with collagen is very limited. To date, theories of mineral/collagen relationships have focused on the potential space presumed to be available within the gap zone as a result of the D-stagger of collagen molecules [3, 13, 23]. Therefore, apatite is generally believed to be excluded from the overlap zones during the early stages of the mineralization process. Evidence to support this viewpoint comes from electron microscopic [24], electron diffraction [25], neutron diffraction, and x-ray diffraction studies [11]. However, recent studies on the specific and direct visualization of apatite by SADF imaging and Fourier-filtered image analysis have shown crystals to be present in both gap and overlap zones at the earliest detectable stages of mineralization in the turkey leg tendon [14–16]. As an extension of this work, the present study compares apatite localization to the molecular orientation and the primary structure of amino acids of type I collagen, and consequently offers an alternative hypothesis of collagen influence on mineral deposition. We observed early stages of intrafibrillar mineralization to be characterized by an asymmetric and subperiodic distribution of apatite crystals which corresponds to specific regions along the N- to C- orientation of the collagen fibril. Both bright field and selected-area dark field imaging revealed mineral within the gap zone to be bordered on either side by discreet nonmineralized areas. Also, a nonmineralized area within the gap zone was invariably positioned nearer the N-terminal direction of the fibril. Mineral within the midportion of the overlap zone was evident from the earliest stages of mineralization. It was concluded from these observations that the heterogeneous distribution of apatite crystals within the gap and overlap zones most likely reflects periodic properties of the collagen fibril within both zones. The regions of low apatite concentration correlate in position and density to computer models depicting the periodic distribution of hydrophobic amino acids (Figs. 4–6). These findings provide evidence for a more complicated distribution of apatite crystals in collagen than simply confined to the gap zones. Thus, we are proposing that in the turkey leg tendon, hydrophobicity is involved in the mechanism of collagen mineralization as a result of apatite restricted from these domains.

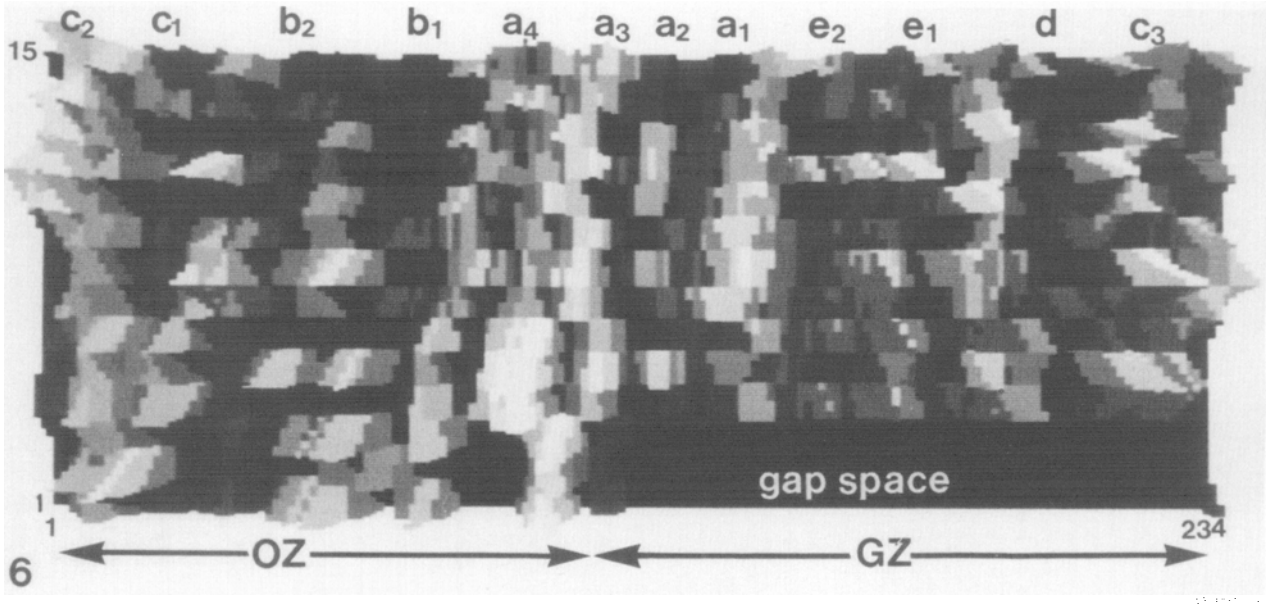

Fig. 6. A three-dimensional representation of local variations in hydrophobicity within a single D repeating unit. In this perspective, the position and degree of hydrophobicity are viewed from above with white representing the highest levels and black the lowest. The long axis is labeled according to the PTA/UA staining pattern (e to a) for orientation purposes and represents the amino acid position in the peptide chain starting at the positions adjacent to the N- terminus. The width of the image represents peptides, number 1–15, assuming that these peptides are linear rather than in a triple helical conformation. For graphic purposes, the width of each molecule and the gap space are both greatly overrepresented. From this 3-D graphics presentation, three regions of high hydrophobicity are observed to span the width of the D unit—two regions in the overlap zone (OZ), c_2-c_1 and a_4-a_3, and one in the gap zone (GZ), a_1-e_2. Other regions of both zones vary in levels of hydrophobicity across the D unit giving a highly textured appearance. The spatial distribution of low hydrophobic levels (black to dark grey pixels) corresponds to the sites of early mineral deposition in both the overlap zone and the gap zone.

This work has a number of implications on the interrelationship between the mechanism of collagen mineralization and the architecture of apatite crystal distribution as defined by the molecular ordering of collagen.

Specific regions localized along the collagen molecule are high in hydrophobic amino acids (a_4-a_3, c_2-c_1, and a_1-e_2) and correlate to areas that may inhibit crystal formation or prevent crystal growth (Figs. 4 and 5). Conversely, mineral distribution can be expected to occur in regions with less spatial density of hydrophobic amino acids. We are speculating that the hydrophobic effect may influence either of two processes. First, the initial site of nucleation may be determined by a specific environment isolated from the hydrophobic areas. For example, the diffusion and localization of various ions including calcium and phosphate will be affected by the close association of hydrophobic groups. Local concentration gradients of these ions are likely to be critical for the nucleation of biological apatite. Also, properties of the collagen fibril may be instrumental in the localization of noncollagenous molecules which have negative or positive control on crystal growth. Macromolecules, such as proteoglycans [26], have specific sites of association with collagen. Various macromolecules including phosphoproteins [27], γ-carboxyglutamic acid [28], and osteocalcin [29] have been associated with collagen-rich mineralizing tissues. Secondly, apatite crystal size and growth may be influenced by space and energy requirements. The dissociation of hydrophobic groups during the mineralization process will require a net energy that will affect the distribution of mineral, the result being that areas of hydrophobicity may compartmentalize regions of optimal crystal growth. Both of these two processes, whether local environmental conditions or energy considerations, occur as a result of the favorable free energy state achieved by minimizing the interaction of hydrophobic groups with the aqueous medium [30]; and neither is mutually exclusive. In addition, these potential processes do not exclude concurrent influences.

Electron microscopic imaging of calcified tissues represents a technical challenge to maintain and detect the mineral component while relating this to the organic matrix. For example, the detection of electron-lucent regions is dependent on the degree of mineralization, the thickness of the specimen, the size of the region, and the angle of incident electrons. If we estimate the thickness of the specimen

to be 70 nm and the predicted size of the hydrophobic regions based on computer models (a_4-a_3 = .12D or about 7.8 nm, c_2-c_1 = .14D or about 9.4 nm, and a_1-e_2 = .07D or about 4.7 nm) and assume the entire thickness is mineralized then we can estimate a critical angle of electron incidence at which these regions will be no longer detectable. At an incidence angle of approximately 3.5°, the space within the gap zone would be obscured. Thus, one can expect few consecutive D periods to show evidence of these regions because of variations in fibril orientation. A further complication of specimen thickness is that distortions in the three-dimensional structure of collagen [31] contributes to misinterpretations of crystal-collagen spatial relationships. In addition, current methods used to quantify mineral content within small regions have limited sensitivity. Modifications of current techniques are required to unambiguously visualize the organic matrix while preserving the mineral component. The staining of collagen with UA in alcohol is an alternative approach to the demineralizing effects of aqueous PTA/UA stains but produces a different collagen banding pattern (Figs. 1 and 3).

In conclusion, we have observed an asymmetric and subperiodic distribution of apatite crystals within the collagen fibril which corresponds to its molecular orientation. This mineral distribution has a reverse correlation to the position of hydrophobic groups as determined by computer modeling and may reflect intrinsic properties of collagen structure throughout the gap and overlap zones. Therefore, we believe further study of mineral/collagen interactions should consider the entire D period of collagen, rather than focus solely on the potential space within the gap zone. In fact, with further analysis using this computer modeling system we have observed the apatite distribution to occur in areas of the D unit having low concentrations of proline and hydroxyproline; this correlates with areas having a high potential for molecular flexibility (Maitland and Arsenault, unpublished data). The application of this computer modeling system should prove to be an extremely useful tool for studying single or multiple properties of collagen which would potentially influence the growth and deposition of mineral. Such physical/chemical influences would be the sites of potential space, hydrophobicity, molecular flexibility, cross-linkages, point mutations, and the distributions of collagen-associated proteins and proteoglycans.

Acknowledgments. The major portion of this work was done at the Department of Anatomy, University of British Columbia and was supported by a grant and scholarship from the Medical Research Council of Canada (to ALA) and a Physiotherapy Foundation of Canada Scholarship (to MEM). Mr. Maitland completed this work as a partial requirement for a Master's thesis in the Department of Anatomy, University of British Columbia.

References

1. Piez K, Eigner E, Lewis M (1963) The chromatographic separation and amino acid composition of the subunits of several collagens. Biochemistry 1:58–66
2. Veis A (1985) Molecular structure and models of collagen fibril assembly. In: Reddi AH (ed) Extracellular matrix structure and function. Alan R Liss, New York, pp 351–358
3. Hodge AJ, Petruska JA (1963) Recent studies with the electron microscope on ordered aggregates of the tropocollagen macromolecule. In: Ramachandran GN (ed) Aspects of protein structure. Academic Press, New York, pp 289–300
4. Hulmes KJS, Miller A, Parry DAD, Piez KA, Woodhead-Galloway J (1973) Analysis of the primary structure of collagen for the origins of molecular packing. J Mol Biol 79:137–148
5. Bear RS (1952) The structure of collagen fibrils. Adv Protein Chem 7:69–160
6. Meek KM, Chapman JA, Hardcastle RA (1979) The staining pattern of collagen fibrils: improved correlation with sequence data. J Biol Chem 254:10710–10714
7. Tzaphilidou M, Chapman JA, Meek KM (1982) A study of positive staining for electron microscopy using collagen as a model system-I. Staining by phosphotungstate and tungstate ions. Micron 13:119–131
8. Tzaphilidou M, Chapman JA, Al-Samman MH (1982) A study of positive staining for electron microscopy using collagen as a model system-II. Staining by uranyl ions. Micron 13:133–145
9. Chapman JA, Hulmes DJS (1984) Electron microscopy of the collagen fibril. In: Ruggeri A, Motta PM (eds) Ultrastructure of the connective tissue matrix. Martinus Nijhoff, Boston, pp 1–33
10. Meek KM, Chapman JA (1985) Glutaraldehyde-induced changes in the axially projected fine structure of collagen fibrils. J Mol Biol 185:359–370
11. White SW, Hulmes DJS, Miller A, Timmins PA (1977) Collagen-mineral axial relationship in calcified turkey leg tendon by x-ray and neutron diffraction. Nature 266:421–425
12. Berthet-Colominas C, Miller A, White SW (1979) Structural study of the calcifying collagen in turkey leg tendons. J Mol Biol 134:431–445
13. Glimcher MJ (1985) The role of collagen and phosphoproteins in the calcification of bone and other collagenous tissues. In: Rubin RP, G Weiss, JW Putney Jr (eds) Calcium in biological systems. Plenum, New York, pp 607–616
14. Arsenault AL (1988) Crystal-collagen relationships in calcified turkey leg tendons visualized by selected-area dark field electron microscopy. Calcif Tissue Int 43:202–212
15. Arsenault AL (1989) A comparative electron microscopic study of apatite crystals in collagen fibrils of rat bone, dentin and calcified turkey leg tendons. Bone Miner 6:165–177
16. Arsenault AL (in press) Image analysis of collagen-associated mineral distribution in cryogenically prepared turkey leg tendons. Calcif Tissue Int
17. Highberger JH, Corbett C, Dixit SN, Wing Y, Jerome MS, Kang AH, Gross J (1982) Amino acid sequence of chick skin collagen α1(I)-CB8 and the complete primary structure of

the helical portion of the chick skin collagen α1(I) chain. Biochemistry 21:2048–2054
18. Boedtker H, Finer M, Sirpa A (1985) The structure of the chicken α2 collagen gene. In: Fleischmajer R, Olsen BR, Kuhn K (eds) The biology, chemistry and pathology of collagen. Ann NY Acad Sci 460:85–116
19. Hofmann H, Fietzek PP, Kuhn K (1978) The role of polar and hydrophobic interactions for the molecular packing of type I collagen: a three-dimensional evaluation of the amino acid sequence. J Mol Biol 125:137–165
20. Kyte J, Doolittle RF (1982) A simple method for displaying the hydropathic character of a protein. J Mol Biol 157:105–132
21. Hodge AJ, Schmitt FO (1960) The charge profile of the tropocollagen macromolecule and the packing arrangement in native-type collagen fibrils. Proc Natl Acad Sci 46:186–197
22. Arsenault AL, Hunziker EB (1988) Electron microscopic analysis of mineral deposits in the calcifying epiphyseal growth plate. Calcif Tissue Int 42:119–126
23. Miller A (1984) Collagen: the organic matrix of bone. Phil Trans R Soc Lond B 304:455–477
24. Glimcher MJ (1959) Molecular biology of mineralized tissues with particular reference to bone. Rev Mod Phys 31:359–393
25. Engström A (1966) Apatite-collagen organization in calcified tendon. Exp Cell Res 43:241–245
26. Scott JE, Haigh M (1985) Proteoglycan-type I collagen fibril interactions in bone and non-calcifying connective tissues. Biosci Rep 5:71–81
27. Veis A (1985) Phosphoproteins of dentin and bone: do they have a role in matrix mineralization? In: Butler WT (ed) The chemistry and biology of mineralized tissues. Ebsco Media, Birmingham, Alabama, pp 170–176
28. Glimcher MJ, Brickley-Parson D, Kossiva D (1979) Phosphoproteins and γ-glutamic acid-containing peptides in calcified turkey tendon: their absence in uncalcified tendon. Calcif Tissue Int 27:281–284
29. Hauschka PV, Lian JB, Gallop PM (1975) Direct identification of the calcium-binding amino acid γ-carboxyglutamate in mineralized tissue. Proc Natl Acad Sci USA 72:3925–3929
30. Tanford C (1980) The hydrophobic effect: formation of micelles and biological membranes, 2nd ed. John Wiley and Sons, New York
31. Hulmes DJS, Holmes DF, Cummings C (1985) Crystalline regions in collagen fibrils. J Mol Biol 184:473–477

Received July 28, 1989, and in revised form December 29, 1989